Development of Electrochemical Aptasensor for Label-Free Glioma Cell Detection

Xianjun Zhao[1], Rongjin Fang[2] and Yunfeng Zhang[3,*]

[1] Department of Neurosurgery, The Second Hospital of Lanzhou University, Lanzhou, Gansu, 730030, P.R. China.
[2] Department of Neurosurgery, Ankang Hospital of Traditional Chinese Medicine, Ankang, Shaanxi, 725000, P.R. China.
[3] Department of Neurosurgery, The Chinese people's Liberation Army Navy Anqing Hospital, Anqing, Anhui, 246003, P.R. China
[*]E-mail: zhang_yunfeng0709@foxmail.com

This work explored the fabrication of a functionalized graphene-and-aptamer AS1411-based electrochemical sensor to achieve tag-free cancer cell determination. The proposed electrochemical aptasensor could distinguish between normal cells and glioma cells with a low detection limit due to the excellent binding affinity and specificity of AS1411 to the overexpressed nucleolin on the surface of the glioma cells.

1. INTRODUCTION

Annually, the number of individuals diagnosed with cancer is recorded as more than 11 million, which is estimated to increase to 16 million by 2020. Among the primary brain tumours, malignant gliomas are considered the most common, with an annual incidence of 5/100,000 individuals [1, 2]. Bailey and Cushing classified gliomas for the first time. The classification of glioma applied so far is the version provided by the World Health Organization (WHO), where oligo-astrocytomas (mixed gliomas), ependymomas, oligodendrogliomas and astrocytomas are set as the sub-branches of gliomas. Based on the tumour size, the magnitude of penetration and spread into the lymph nodes or other adjacent or distant organs, the tumours are potentially divided into varied stages for more convenient classification; thus, the TNM staging system is constructed. Herein, the three

letters respectively represent tumour, lymph nodes and metastasis. Hence, five stages have been proposed until now.

Aptamers (Apt), single-stranded nucleic acid molecules derived from random single-stranded nucleic acid sequence pools, were selected through the SELEX (Systematic Evolution of Ligands by Exponential Enrichment) process [3, 4]. In comparison with antibodies, aptamers exhibit an increase in reproducibility and thermal stability. And in comparison with other biological therapeutics, they exhibit a reduced toxicity and immunogenicity. Meanwhile, they are potentially produced through solid-phase synthesis. Furthermore, aptamers are significantly affinitive and specific to metal ions [4, 5] and small chemicals [6], large proteins [7-9], whole cells [10, 11] and many other forms of targets. Hence, after being combined with the targets through electrostatic, hydrogen bonding, hydrophobic interactions (occasionally) and many other forms of acting forces [12], it is natural for the aptamers to fold into specific 3-D conformations. It is suitable for aptamers and their nanoparticles (NPs) conjugates to have cell applications in therapeutics, diagnostics and other fields due to their significant selectivity. Flow cytometric analysis [13] was employed by Tan et al. to provide an extensive platform based on a range of Apt-NPs conjugates for the identification of the emerging molecular formation to realize specific cell determination. The utilization of Apt-NPs conjugates for multiple cancer cell collection and detection have also been extended by them [14]. A class of Apt-NPs for cancer cell recognition and therapeutical targeting was developed by Jong et al., where 3–4 times improvement in growth inhibition efficiency was exhibited in comparison with the only use of DNA aptamers [15].

An increasing number of aptamer-based electrochemical sensors have been proposed and developed recently [16-19]. They possess the integrated features of aptamers like desirable affinity and specificity and those of electrochemical sensors like miniaturized commercial detectors, inexpensiveness, convenient use, excellent sensitivity and instant response. Essentially, the variations in aptamer structure [20, 21] and the formation of sandwich structure [22] were characterised for determination, with the main techniques of electrochemical impedance spectroscopy [23] and electrochemical stripping [24, 25]. The latter technique features excellent sensitivity due to the 'built-in' pre-concentration stage during electrodeposition; thus, it has gained particular use for metal-nanoparticle label determination [26].

Graphene is a one-atom-thick planar sheet of sp^2-bonded carbon atoms; it features excellent and ballistic electron transfer [27], half-integer quantum Hall effect and other distinguishing traits and has been the focus of attention in material science recently, where outstanding developments have been made in its application to nanocomposites and nanoelectronics [28]. In addition, graphene also has applications in biological systems like drug delivery carrier and cell/bacterial nanodevice design and protein/pathogen and metal ion/DNA determination [29, 30]. A more extended and non-cytotoxic surface for biomolecule immobilization could be achieved and electron transportation could be facilitated by the graphene-modified electrode due to the high special surface area and the excellent electron transportation features of graphene. Thus, perylene tetracarboxylic acid (PTCA) functionalized graphene-modified electrode and AS1411 (the first clinical trial II used aptamer for potential cancer treatment) were employed to fabricate an electrochemical aptasensor to realize the sensitive, selective and tag-free determination of cancer cells.

This work explored the fabrication of a reusable graphene-and-aptamer AS1411-based electrochemical aptasensor to determine tag-free glioma cells. As a water-soluble derivative of perylene, 3,4,9,10-perylene tetracarboxylic acid (PTCA) could firmly adsorb onto the graphene via π–π stacking. The graphene was prevented from aggregating by hydrophobic interactions; then, there would be an increase in the amount of negatively-charged –COOH groups on the surface of graphene. A carbodiimide-mediated wet-chemistry approach was employed to link the obtained PTCA-functionalized chemical converted graphene (PTCA/CCG) with the NH_2-modified aptamer strand. Under the specific binding between the aptamer AS1411 and cell surface nucleolin, the cells could be effectively captured on the electrode surface by the terminal aptamer-PTCA nanocomposite as nanoscale anchorage substrate.

2. EXPERIMENTS

2.1. Chemicals

XF Nano Inc. (Nanjing, China) was the material source for graphite oxide. Acridine orange (AO) dye, (3-aminopropyl) triethoxysilane (APTES) (98%), Tris(hydroxymethyl) aminomethane (Tris), 2-(N-morpholino) ethanesulfonic acid (MES), Nafion, N-hydroxysuccinimide (NHS), 1-ethyl-3-(3-dimethylaminopropyl) carbodiimide (EDC) and 3,4,9,10-perylene tetracarboxylic dianhydride were commercially available in Sigma. The Chinese people's Liberation Army Navy Anqing Hospital provided the glioma cells. All oligonucleotides were synthesized by Sangon Biotechnology Co. (Shanghai, China). All other reagents were of analytical grade and employed as obtained. Super-pure water (≥18 MΩ, Milli-Q, Millipore) was employed to prepare all aqueous solutions.

2.2. PTCA/CCG and CCG synthesis

In general, after the hydrolyzation of 3,4,9,10-perylene tetracarboxylic dianhydride (PTCAD) in sodium hydroxide (roughly 100 μl, 1m), a PTCA solution in yellow-green was obtained. It was then centrifugalized and collected in solid form, which was then dried at 37 °C under vacuum. PTCA powder (5.0 mg) was added to GO solution (1 mL, 1.5 mg/ml), with H_2O added up to 20 mL. After being ultrasonicated for 60 min, the obtained mixture was left stirring overnight at 40 °C. This mixed solution was then added with hydrazine solution (15 μl) and ammonia solution (30 μl) and finally left under vigorous stirring for 30 min at 90 °C. Similar procedures were employed to prepare the CCG solution, except for the absence of PTCA as a stabilizer in the course of reduction.

2.3. Electrode fabrication

After successive polishing with alumina (1.0, 0.3, and 0.05 μm), the obtained glassy carbon electrodes (GCE) were kept under sonication for 3 min prior to modification. The mixture of PTCA/CCG solution and 0.1% Nafion solution (4:1) was aimed at improving the affinity of

composites to GCE. Subsequently, the obtained PTCA/CCG-Nafion solution (5 μL) was dropped on the pretreated GCE and dried at 37 °C. This was followed by casting the activation solution onto the surface for 60 min for the activation of the carboxyl group and instantly dropping DNA (1 μM) with the terminal amine group onto the surface, which was then kept under incubation for 180 min. Afterwards, the modified surface was buffer washed, hybridized with aptamer DNA (1 μm), and stored in the air before application.

2.4 Cell lines and cell culture

MCF-7 cells (human glioma cell), HeLa cells (human Cervix adenocarcinoma) and NIH3T3 cells (mouse embroyonic fibroblast cell line) were obtained from Nanjing KeyGen Biotech Co. Ltd. MCF-7 and HeLa cells were cultured in a flask in DMEM medium (Gibco, Grand Island, NY) supplemented with 10% fetal calf serum, penicillin and streptomycin in an incubator (5% CO_2, 37 °C). The cells were collected from 90% confluent cell culture plates by aspirating off the media and incubating with trypsin for 3-5 min. Five milliliters of media was added to dilute and neutralize the trypsin solution. Then this solution was separated from the medium by centrifugation at 1000 rpm for 10 min and washed twice with a sterile PBS. The sediment was suspended in the PBS to obtain a homogeneous cell suspension with the final concentration of ∼107 cells/mL. The cell suspensions with various contents were prepared from this stock. NIH3T3 cells were cultured in a flask in RPMI 1640 medium (Gibco, Grand Island, NY) supplemented with the same as other cells.

2.5. Apparatus and characterization

A CHI 660a workstation (Shanghai Chenhua, Shanghai) with a traditional triple-electrode configuration was employed for electrochemical assays in PBS solution (pH 7.4) containing $Fe(CN)_6^{3-/4-}$ (10 mM) and KCl (0.1 M). Herein, the roles of the reference, auxiliary and working electrode were taken by Ag/AgCl, a platinum wire and the modified glassy carbon electrode, respectively. An Autolab PGSTAT12 (Ecochemie, BV) was employed for the Electrochemical Impedance spectroscopy (EIS) measurements with a frequency range of $10^{-1} \sim 10^5$ Hz in PBS solution (10 mM, pH 7.4) containing $Fe(CN)_6^{3-/4-}$ (10 mM) and KCl (0.1 M). A UV-3600 spectrophotometer from Shimadzu (located in Kyoto) and a BRUKE Vertex 70 FT-IR spectrometer were employed for UV–vis and FT-IR measurements, respectively.

3. RESULTS AND DISCUSSION

It was found that PTCA was significantly adsorbed onto the graphene surface, as indicated by a red-shift (roughly 80 nm) observed for two UV absorption peaks of PTCA as well as the complete quench of PTCA fluorescence (Fig. 1A and B) upon the adsorption of PTCA onto the graphene sheet surface. The result suspension is black with a little violet, and stable for several months at room temperature.
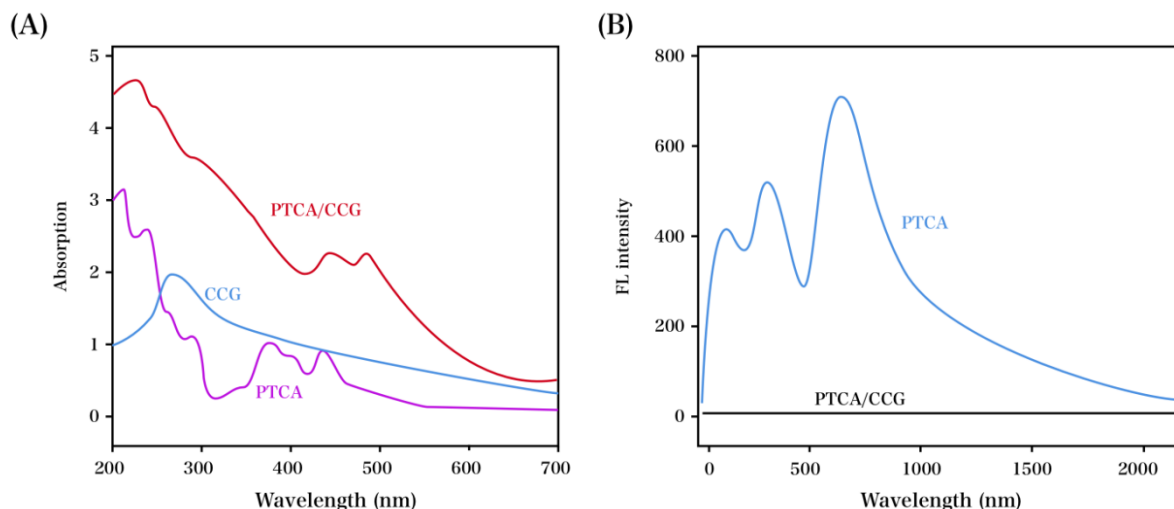
Figure 1. (A) Absorption spectra of PTCA, PTCA-functionalized graphene (PTCA/CCG) and chemical converted grapheme (CCG) in water. (B) Fluorescence spectra of PTCAand PTCA/CCG in water.

The amount of PTCA molecules on graphene is estimated by TGA, as indicated in Fig. 2. The carbonization of the molecular structure was suggested by thermal decomposition at 800 °C. And the presence of PTCA in the composite specimens is reflected by the 15.4% mass loss between CCG and PTCA/CCG [31]. Furthermore, the graphene-quenched PTCA fluorescence as well as the significant hydrophobic and π-π stacking interactions found between CCG and PTCA were well indicated by all the TGA and spectroscopic results.
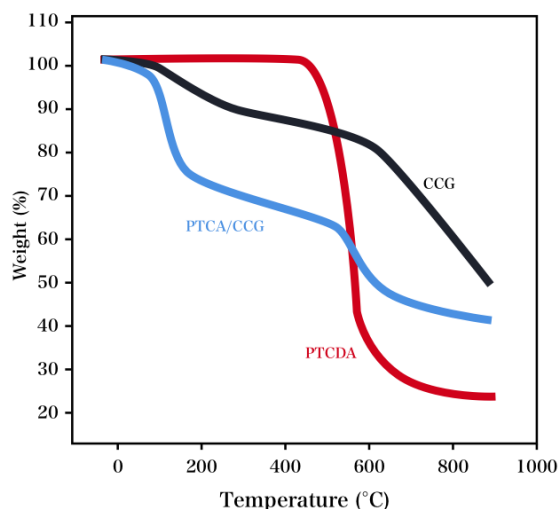
Figure 2. TGA profiles of PTCA, PTCA-functionalized graphene (PTCA/CCG) and chemical converted grapheme (CCG).

As an outstanding technique to monitor the variations of interfacial features on the electrode surface, EIS was employed in this work. Its Nyquist plot consists of a straight line in the low-

frequency domain and a semicircle in the high-frequency domain, with mass transfer represented by the former and capacitance and resistance characterized by the latter. Herein, the electro-transfer resistance (R_{et}) is consistent with the diameters of the semicircle. EIS addressed the characterization of the construction process and exhibited pronounced variations in the course of modification. As indicated in Fig. 3A, a nearly straight line was shown for the GCE, where a fast electron-shift process was exhibited for $Fe(CN)_6^{3-/4-}$. An increase was observed for the electron-shift resistance as the aptamer was immobilized, mostly attributed to the electrostatic repulsion between the $Fe(CN)_6^{3-/4-}$ probe and negative charges of the aptamer. Further impedance of the redox probe of $[Fe(CN)6]^{3-/4-}$ in the vicinity of the electrode surface and increase in the electron-shift resistance can be caused by the cancer cell binding. This demonstrated that a cancer cell was assembled onto the electrode. After the aptamer was hybridized with a cancer cell, a further increase in Ret could be observed because negatively charged aptamer could repel the negative charged redox probe $Fe(CN)_6^{3-/4-}$, and thus the interfacial electron transfer resistance was increased [32-34]. It can be concluded from the EIS data that immobilization, competitive binding and resolving have been achieved as estimated.

The as-prepared electrode was also characterized via cyclic voltammetry (CV) with the redox probe of $Fe(CN)_6^{3-/4-}$ after each modification stage. The original GCE exhibited a couple of well-defined redox peaks (Fig. 3B), where the electron-shift kinetics of $Fe(CN)_6^{3-/4-}$ was found to be prominent. After the assembly of aptamer and glioma cells to the as-prepared electrode, an obvious increase was observed for the peak-to-peak potential separation, together with a reduction in the amperometric response. Thus, it could be concluded that the interfacial electron shift was enhanced in irreversibility. When aptamer and PTCA/CCG were combined with the electrode surface, similar phenomena were obtained. However, upon being incubated with the glioma cell, a competitive reaction took place on the electrode surface, which resulted in a peak current increase [35-37]. The consistency between EIS variations and CV performances further proved that the modification was successfully conducted, and the competition was shown as expected.
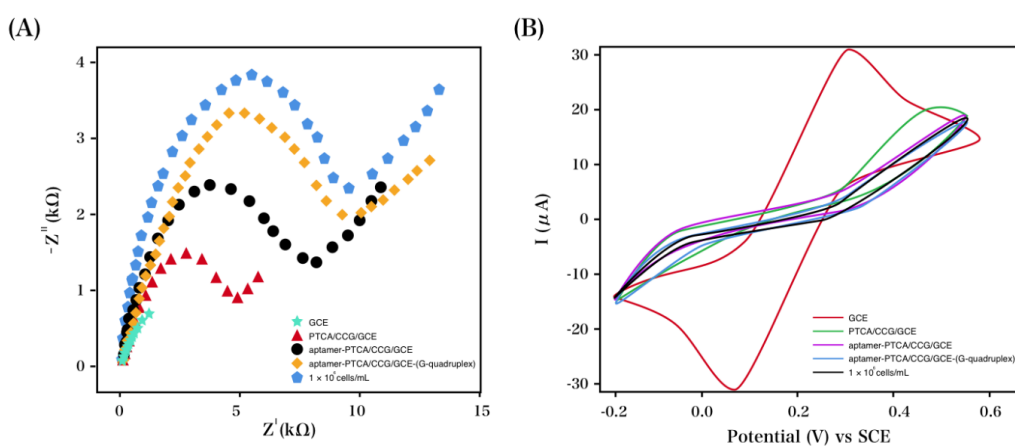
Figure 3. (A) Nyquist profiles electrochemical impedance spectra of $[Fe(CN)_6]^{3-/4-}$ and (B) CV at: GCE, PTCA/CCG/GCE; aptamer-PTCA/CCG/GCE, aptamer-PTCA/CCG/GCE-(G-quadruplex) and 1×10^6 cells/mL at the electrode.
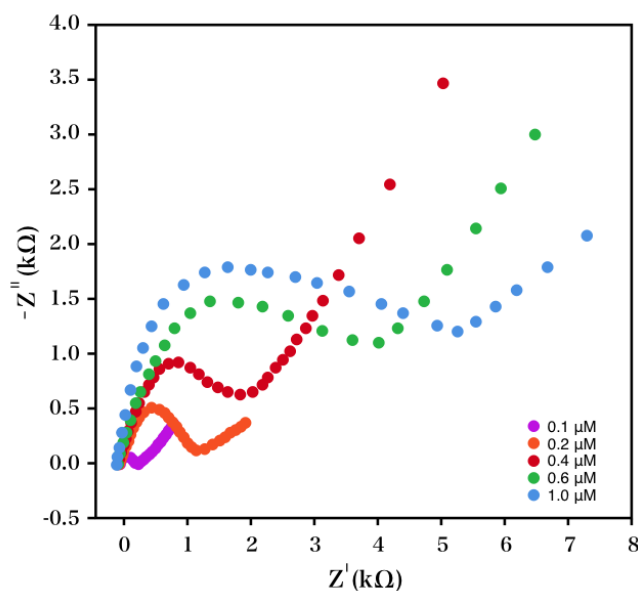
Figure 4. Nyquist profile of electrochemical impedance spectra recorded in a range of 0.1 to 10^5 Hz for $[Fe(CN)_6]^{3-}/[Fe(CN)_6]^{4-}$ (10 mM, 1:1) in 0.1 M KCl at PTCA/CCG/GCE with the aptamer amount of 0.1, 0.2, 0.4, 0.6 and 1.0 μM.

As the aptamer at the modified electrode increased, there was a rise in the stripping peak current, which then reached a plateau. The concentration of the aptamer was taken into consideration to achieve optimal conditions. Fig. 4 indicated a gradual increase and finally a plateau for the R_{et} of the electrode with the increase in aptamer concentration, indicating that increasing the number of aptamers could be immobilized onto the electrode surface with saturated binding obtained at 1 μM. Thus, 1μM was selected to guarantee a thoroughly saturated binding in further measurements.

A semilogarithmic dependence observed between the glioma cell concentration and R_{et} (Fig. 5A) indicates the dependence of the impedance increase on the surface coverage of cells. Herein, the detection range is obtained as 1×10^3 to 1×10^6 cells/mL, with a correlation coefficient R of 0.988 and a detection limit of 750 cells/mL at 3σ, which was comparable to those reported by most aptamer-based assays [38] and other electrochemical and fluorescence cytosensing strategies for cancer cell detection [39, 40]. EIS assays are employed for the comparison of four varied cell lines. Upon the respective incubations with K562, MDA-231 and HeLa cells of the same concentration (1×10^5 cells/mL), there was a significant increase in R_{et} observed for the electrode. Nevertheless, in contrast to cancer cells, the normal NIH3T3 cells exhibited an insignificant increase in R_{et} values under the same conditions (Fig. 5B), indicating the significant binding affinity of AS1411 to the overexpressed nucleolin on the surface of the cell in contrast to normal cells [41-43]. Hence, it can be concluded that the differentiation between normal cells and cancer cells can be realized by the proposed electrochemical aptasensor.
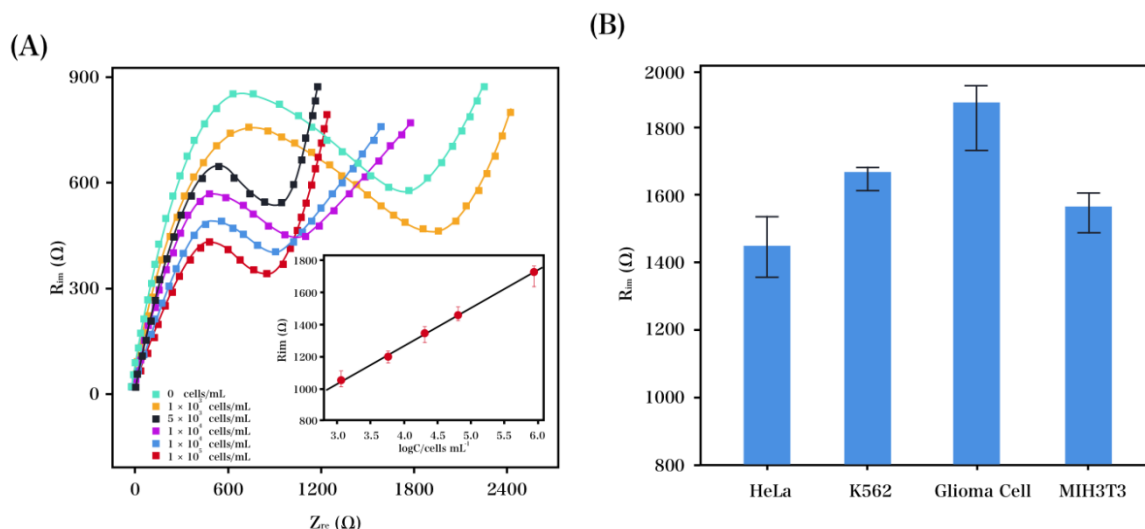
Figure 5. (A) Nyquist profiles of the obtained GCE after the immersion in 0, 1×10^3, 5×10^3, 1×10^4, 1×10^5 and 1×10^6 cells/mL glioma cell suspension. Inset: the linear relationship between R_{et} and logarithm of glioma cell concentration. (B) Selectivity analysis for cancer cell determination via the surveillance of the R_{et} value between three types of cancer cell lines, HeLa cells, K562 cells, glioma cells and normal cell line, NIH3T3 cells.

MTT measurement exhibited no pronounced cytotoxicity for the PTCA/CCG nanocomposite. Furthermore, to work out whether the film is non-cytotoxic, the growth and proliferation of glioma cells on the aptamer-modified graphene surface were monitored and evaluated. Glioma cells can adhere to the film as well as grow and proliferate on it. After being incubated for 8 h, the originally round cells that nearly adhered grew into irregular shapes on the film surface. After incubation for 3 d, the adhered cells were still desirably viable, as indicated by the AO dye molecules-engaged fluorescent stain and cellular morphology. Under our test conditions, the non-cytotoxicity of the aptamer-designed graphene surface is therefore evidenced.

4. CONCLUSIONS

This work addressed the fabrication of a functionalized graphene-and-aptamer AS1411-based electrochemical sensor to achieve the determination of tag-free glioma cells. Herein, no cytotoxicity is exhibited for the as-prepared graphene surface, as indicated in the significant binding affinity and specificity of the AS1411-formed G-quadruplex on the surface of the glioma cells in contrast to normal ones. Therefore, the as-prepared electrochemical aptasensor can potentially be employed for differentiation between normal cells and cancer cells.

References

1. D. Louis, H. Ohgaki, O. Wiestler, W. Cavenee, P. Burger, A. Jouvet, B. Scheithauer and P.

Kleihues, *Acta Neuropathologica*, 114 (2007) 97.

2. P. Wen and S. Kesari, *N. Engl. J. Med.*, 359 (2008) 492.
3. A. Ellington and J. Szostak, *Nature*, 355 (1992) 850.
4. C. Tuerk and L. Gold, *Science*, 249 (1990) 505.
5. C. Lin and D. Patei, *Chemistry & Biology*, 4 (1997) 817.
6. D. Zheng, D. Seferos, D. Giljohann, P. Patel and C. Mirkin, *Nano Letters*, 9 (2009) 3258.
7. A. Higuchi, Y. Siao, S. Yang, P. Hsieh, H. Fukushima, Y. Chang, R. Ruaan and W. Chen, *Anal. Chem.*, 80 (2008) 6580.
8. Y. Kang, K. Feng, J. Chen, J. Jiang, G. Shen and R. Yu, *Bioelectrochemistry*, 73 (2008) 76.
9. M. Mir, A. Jenkins and I. Katakis, *Electrochemistry Communications*, 10 (2008) 1533.
10. D. Shangguan, Y. Li, Z. Tang, Z. Cao, H. Chen, P. Mallikaratchy, K. Sefah, C. Yang and W. Tan, *Proceedings of the National Academy of Sciences*, 103 (2006) 11838.
11. C. Hamula, H. Zhang, L. Guan, X. Li and X. Le, *Anal. Chem.*, 80 (2008) 7812.
12. R. Miranda-Castro, N. de-los-Santos-Álvarez, M. Lobo-Castañón, A. Miranda-Ordieres and P. Tuñón-Blanco, *Electroanalysis*, 21 (2009) 2077.
13. H. Wang, R. Yang, L. Yang and W. Tan, *ACS Nano*, 3 (2009) 2451.
14. J. Smith, C. Medley, Z. Tang, D. Shangguan, C. Lofton and W. Tan, *Anal. Chem.*, 79 (2007) 3075.
15. J. Choi, K. Chen, J. Han, A. Chaffee and M.S. Strano, *Small*, 5 (2009) 672.
16. I. Willner and M. Zayats, *Angewandte Chemie International Edition*, 46 (2007) 6408.
17. H. Huang, G. Jie, R. Cui and J. Zhu, *Electrochemistry Communications*, 11 (2009) 816.
18. K. Feng, Y. Kang, J. Zhao, Y. Liu, J. Jiang, G. Shen and R. Yu, *Analytical Biochemistry*, 378 (2008) 38.
19. B. Baker, R. Lai, M. Wood, E. Doctor, A. Heeger and K. Plaxco, *Journal of the American Chemical Society*, 128 (2006) 3138.
20. J. Liu, Z. Cao and Y. Lu, *Chemical Reviews*, 109 (2009) 1948.
21. E. Ferapontova, E. Olsen and K. Gothelf, *Journal of the American Chemical Society*, 130 (2008) 4256.
22. A. Numnuam, K. Chumbimuni-Torres, Y. Xiang, R. Bash, P. Thavarungkul, P. Kanatharana, E. Pretsch, J. Wang and E. Bakker, *Anal. Chem.*, 80 (2008) 707.
23. X. Li, L. Shen, D. Zhang, H. Qi, Q. Gao, F. Ma and C. Zhang, *Biosensors and Bioelectronics*, 23 (2008) 1624.
24. J. Hansen, J. Wang, A. Kawde, Y. Xiang, K. Gothelf and G. Collins, *Journal of the American Chemical Society*, 128 (2006) 2228.
25. Y. Huang, X. Nie, S. Gan, J. Jiang, G. Shen and R. Yu, *Analytical Biochemistry*, 382 (2008) 16.
26. J. Wang, *small*, 1 (2005) 1036.
27. C. Rao, A. Sood, K. Subrahmanyam and A. Govindaraj, *Angewandte Chemie International Edition*, 48 (2009) 7752.
28. M. Allen, V. Tung and R. Kaner, *Chemical Reviews*, 110 (2009) 132.
29. H. Postma, *Nano Letters*, 10 (2010) 420.
30. Y. Wen, F. Xing, S. He, S. Song, L. Wang, Y. Long, D. Li and C. Fan, *Chemical Communications*, 46 (2010) 2596.
31. Q. Wang and M. Hersam, *Nature Chemistry*, 1 (2009) 206.
32. Y. Borghei, M. Hosseini, M. Dadmehr, S. Hosseinkhani, M. Ganjali and R. Sheikhnejad, *Anal. Chim. Acta.*, 904 (2016) 92.
33. X. Zhang, K. Xiao, L. Cheng, H. Chen, B. Liu, S. Zhang and J. Kong, *Anal. Chem.*, 86 (2014) 5567.
34. H. Shi, M. Wu, Y. Du, J. Xu and H. Chen, *Biosensors and Bioelectronics*, 55 (2014) 459.
35. Q. Zhou, T. Kwa, Y. Gao, Y. Liu, A. Rahimian and A. Revzin, *Lab on a Chip*, 14 (2014) 276.
36. P. Gai, C. Gu, T. Hou and F. Li, *Anal. Chem.*, 89 (2017) 2163.
37. B. Yuan, Y. Zhou, Q. Guo, K. Wang, X. Yang, X. Meng, J. Wan, Y. Tan, Z. Huang and Q. Xie,

Chemical Communications, 52 (2016) 1590.
38. C. Pan, M. Guo, Z. Nie, X. Xiao and S. Yao, *Electroanalysis*, 21 (2009) 1321.
39. M. Xie, J. Hu, Y. Long, Z. Zhang, H Xie and D. Pang, *Biosensors and Bioelectronics*, 24 (2009) 1311.
40. X. Zhang, S. Li, X. Jin and X. Li, *Biosensors and Bioelectronics*, 26 (2011) 3674.
41. P. Bates, J. Kahlon, S. Thomas, J. Trent and D. Miller, *Journal of Biological Chemistry*, 274 (1999) 26369.
42. V. Đapić, V. Abdomerović, R. Marrington, J. Peberdy, A. Rodger, J. Trent and P. Bates, *Nucleic Acids Research*, 31 (2003) 2097.
43. S. Soundararajan, L. Wang, V. Sridharan, W. Chen, N. Courtenay-Luck, D. Jones, E. Spicer and D. Fernandes, *Molecular Pharmacology*, 76 (2009) 984.